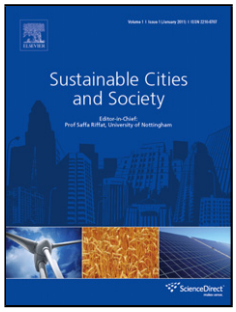

Title: Effects of Urban Heat Island Mitigation in Various Climate Zones in the United States

Authors: Hyoungsub Kim, Donghwan Gu, Hwan Yong Kim

PII: S2210-6707(18)30132-X
DOI: https://doi.org/10.1016/j.scs.2018.06.021
Reference: SCS 1155

To appear in:

Received date: 22-1-2018
Revised date: 15-6-2018
Accepted date: 16-6-2018

Please cite this article as: Kim H, Gu D, Kim HY, Effects of Urban Heat Island Mitigation in Various Climate Zones in the United States, *Sustainable Cities and Society* (2018), https://doi.org/10.1016/j.scs.2018.06.021

Title

Effects of Urban Heat Island Mitigation in Various Climate Zones in the United States

1 AUTHORS

Hyoungsub Kim, Ph.D. (First Author)

Department of Architecture, College of Architecture, Texas A & M University, 3137 TAMU, College Station, TX 77843, USA; Email: hskim@tamu.edu

Donghwan Gu

Department of Landscape Architecture and Urban Planning, College of Architecture,

Texas A & M University, 3137 TAMU, College Station, TX 77843, USA; Email: dgu@tamu.edu

Hwan Yong Kim, Ph.D. (Corresponding Author)

Division of Architecture and Urban Design, College of Urban Sciences, Incheon National University, 119 Academy-Ro, Songdo-dong, Yeonsu-Gu Incheon 22012, Korea

Highlights

- Investigation of the UHI effect in different climate zones.
- Development of an urban model using statistical urban district information.
- Investigation of sensitivity of UHI mitigation strategies in different climate zones.
- Analysis of the impact of the UHI on the level of heat stress in different climate zones.

Abstract

This research investigates the Urban Heat Island (UHI) effect in different climate zones in order to analyze the efficacy of UHI mitigation strategies. A base case urban canopy model was developed using statistical urban district information for Houston, Texas. The Urban Weather Generator (UWG) was employed to simulate the UHI effect during the hottest week of the Typical Meteorological Year (TMY3). Two case studies were conducted to represent the impacts of UHIs on the different climate zones. First, a case study was conducted to compare the

UHI effect in various climate conditions. We controlled the urban morphology to estimate the effects of the climate zones on UHIs, but the UHI intensity outcomes still considerably differed from one another, ranging from 1.25□ to 4.35□. Second, UHI mitigation strategies such as roof vegetation, trees, and grass coverage ratio were tested to measure their sensitivity in different climate conditions. The results show that green roofs have a marginal effect on UHI mitigation in high-rise urban morphology, while increases in grass and tree coverage ratios were effective, especially in hot climates. The results also indicate that the strategies employed should consider the climate's characteristics in order to encourage a more sustainable built environment.

Keywords: Urban Heat Island; UHI Mitigation; Climate Zone; Urban Weather Generator (UWG) Simulation

2 INTRODUCTION

The expansion of highly dense built environments and the resulting increase in human activities have led to significant temperature differences between urban and rural areas; this phenomenon has come to be known as Urban Heat Islands (UHIs) (Santamouris, 2013). Urban expansion and the resultant land cover changes that follow the increased energy use are known factors in UHI promotion. Moreover, buildings and their surroundings are major contributors to UHIs, especially in urban cores with high population densities (Arnfield, 2003; Sailor and Lu, 2004). To be specific, UHIs are caused by the stored heat from radiative imbalances, anthropogenic heat emissions, lowered wind speeds, a lack of green surfaces that encourage evaporation, and the material properties of buildings and pavement (Oke et al., 1991; Oke, 1982). These causes have been examined in detail by research addressing urban built environments. Topics of such studies include consumed energy, pollution, heat emissions from human activities in buildings (Hassid et al., 2000; Santamouris et al., 2001; Santamouris et al., 2011), decreased wind speed according to the layout of the built environment (Santamouris et al., 2001), low albedo and Solar Reflectance Index (SRI) levels of the material properties of buildings and pavement (Heidt and Neef, 2008; Santamouris et al., 2011), intensive land use (Harlan and Ruddell, 2011; Mavrogianni et al., 2011), a lack of pervious green surfaces (Chen et al., 2009; Smith and Levermore, 2008), and the resulting loss of stored long-wave radiation (Smith and Levermore, 2008).

UHIs result in a significant increase in a building's required cooling load (Davies et al., 2008). Buildings in urban areas consume more energy for air conditioning than other buildings in suburban areas (Machairas et al., 2014), which can limit efforts at energy savings. According to the definition of "heat island effect" from the Environmental Protection Agency, the annual mean air temperature can be 1°C to 3°C warmer in an urban area with over 1 million in

population than in the surrounding rural area, and the gap can be increased up to 12°C (Environmental Protection Agency, 2017) where UHIs are geographically dependent (Arnfield, 2003). Based on the resistance-capacitance network model, for each 1°C increase in temperature originating from a UHI, a residential building uses an extra 5% of energy for cooling during one summer night in the dense urban center of Toulouse, France (Bueno, Bruno et al., 2012). While UHIs can decrease in heating demand in winter, the increase in cooling demand in summer has exceeded the decreased heating demand since 1970. As a result, the total energy demand has increased by 11% in 21 cities worldwide (Santamouris, 2014b). This intensifies both the UHI effect (Davies et al., 2008; Eto, 1988; Layberry, 2008) and greenhouse gas emissions (Kennedy et al., 2009).

Considering that the majority of the world's population inhabits urban areas (Jansson, 2013) and the UHI effect exists regardless of the size of the city (Busato et al., 2014; Karl et al., 1988), exacerbation of UHIs is an imminent problem that is currently aggravating building energy consumption. Without properly considering UHI mitigation efforts, increases in the cooling demand caused by UHIs will cause up to a 500% increase in CO_2 emissions by 2050 for buildings in city centers, relative to the 2000 values (Kolokotroni et al., 2012). Regional geography and climate scales are vital to assessing UHI mitigation efforts regarding greenhouse warming on individual building and neighborhoods scales (Georgescu et al., 2014). If the UHI level varies according to the regional climate conditions, the efficiency levels of UHI mitigation strategies by region might be inconsistent (Georgescu et al., 2014; Ramamurthy and Bou-Zeid, 2017). In other words, the "all-around" solutions for mitigating the UHI effect may have only limited benefits in different climate conditions (Georgescu et al., 2014).

In an effort to create better urban environments, many studies have addressed the effects of green building assessments (Georgescu, 2015; Gu et al., 2015; Newsham et al., 2009; Shin et al., 2017) and local climatic conditions on UHIs (Stewart and Oke, 2012; Zhao et al., 2014) on city and regional scales. These studies were focused on the variability of UHIs without controlling for different urban built environment settings. Accordingly, the UHI effect continues to be in question, since derived study results are influenced both by urban built environment settings and regional climate factors (Saneinejad et al., 2014). Especially, urban morphologies such as developed urban areas' contiguity and sprawl, both of which are positively related to the UHI effect (Debbage and Shepherd, 2015). To generalize the effects of UHI mitigation strategies by regional climate, experiments should be conducted in a controlled urban built environment setting. Thus, this research has investigated the impacts of different climate conditions on the level of UHI effect and efficiency of UHI mitigation strategies, using an Urban Canopy Model (UCM) to control the built environment settings. The findings of this research will help policymakers to better understand the relationship between climate conditions and the UHI effect

and assist them in making improved choices with regards to geographically appropriate UHI mitigation policies.

3 BACKGROUND

3.1 UHI Mitigation Strategies and Climate Conditions

Most building energy assessment systems are not efficient at estimating regional urban sustainability from individual buildings' energy efficiency and carbon emissions, due to a lack of urban energy efficiency measures (Bourdic and Salat, 2012). To address regional differences, building energy regulation systems have begun including local geographic and climatic parameters (Suzer, 2015). Criteria-based environmental assessment tools such as a building's regulatory system[1] are designed to "assess the issues that influence the performance of the building itself, and, in some cases, to assess the impact of the building on its surrounding" (Horvat and Fazio, 2005). However, most of these certification systems were not developed to address differences in local climate conditions in the initial development stage. Since variations in the local climate could aggravate the UHI effect and undermine building energy performance, most of the building environment assessment tools have adopted adjustable parameters to address diverse climate conditions (Suzer, 2015). As a result, the energy use intensity of certified high performance green buildings does not correlate with outside air temperature as measured by heating degree days (HDD); non-certified buildings use energy more in proportion to HDD (Mohareb et al., 2011). In addition, certified buildings can have a temperature-lowering effect on their surrounding area (Gu et al., 2015; Shin et al., 2017). Certified buildings' mitigation effects on the outside temperature indicate that the criteria employed by building environment assessment tools could be effective in mitigating the UHI effect.

Moreover, mitigation of the UHI effect improves building energy performance, resulting in a substantial energy savings in urban areas (Machairas et al., 2014). The most prominent UHI causes adopted into the building energy assessment systems also serve to underscore the most effective UHI mitigation methods. The use of high albedo materials and shading from trees and structures for buildings (Akbari et al., 2001; Rosenfeld et al., 1998; Takebayashi and Moriyama, 2012) and pavements (Asaeda et al., 1996; Dimoudi et al., 2014), pervious paving and green roofs (Asaeda et al., 1996; Hathway and Sharples, 2012; He and Hoyano, 2010; Liu, 2002; Nakayama and Fujita, 2010; Saneinejad et al., 2011; Saneinejad et al., 2012; Wanphen and Nagano, 2009), building and urban water bodies (Han and Huh, 2008; Kleerekoper et al., 2012; Krüger and Pearlmutter, 2008; Runsheng et al., 2003; Tiwari et al., 1982), and trees and open

[1]For instance, the Building Research Establishment Environmental Assessment Method (BREEAM) in the UK, Leadership in Energy and Environmental Design (LEED) and ENERGY STAR in the U.S., SBTool (formerly known as GBTool) in Canada, the Comprehensive Assessment System for Built Environment Efficiency (CASBEE) in Japan, Green Star in Australia, and the Building Environmental Assessment Method (BEAM) in Hong Kong.

greenspaces (Akbari, 2002; Akbari et al., 2001; Alexandri and Jones, 2008; Rosenfeld et al., 1998; Rydin et al., 2012; Santamouris, 2014a), as well as the harnessing of natural wind (Smith and Levermore, 2008) are all known to be effective strategies for mitigating UHIs. In practice, however, many studies have argued that UHI mitigation strategies might not work equally well around the world, at least in the absence of consideration of the local climate characteristics (Akbari, 2002; Alexandri and Jones, 2008; Georgescu, 2015; Georgescu et al., 2014; Ramamurthy and Bou-Zeid, 2017). For example, the on-average humidity, precipitation, temperature, and wind speed significantly correlate with UHIs (Du et al., 2016; Zhao et al., 2014). Accordingly, for the appropriate UHI mitigation methods to be used worldwide, the local characteristics of various regional climate conditions should be considered.

3.2 Estimation of UHIs

Numerous studies have developed methods and tools for predicting urban climates by integrating modeling with simulation technology (Bruse, 1998; Bueno et al., 2013b; Erell and Williamson, 2006; Oke, 1981). There are three different types of UHIs, based on the heights of measured locations: Urban Surface Layer (USL); Urban Canopy Layer (UCL), which includes the space between ground and mean roof height; and Urban Boundary Layer (UBL), which is above the UCL (see Figure 1) (Kuttler, 2008).

Figure 1. Three different layers for UHI measurement.

Sky View Factor (SVF) represents the ratio of the radiation received by a planar surface to that of an entire hemispheric radiating environment (Oke, 1981). It can be measured as the sky-visible ratio from a reference point on the ground in the USL, considering the weighted factor of the radiative flux density and solar angles (Brown et al., 2001). The SVF in urban areas can be determined using analytical methods, fish-eye photography, global positioning system signals, and Geographic Information System (GIS)-based three-dimensional datasets (Chen et al., 2012). Various methods have been developed that use the SVF to estimate the UHI effect,

addressing the relationship between the SVF and radiation exchange in the UCL (Gál et al., 2009; Unger, 2004, 2008).

As an analytical model, Canyon Air Temperature (CAT) model was presented to estimate urban air temperatures in the UCL that were transformed from rural weather data (Erell and Williamson, 2006). Crawley (2008) proposed an empirical UHI prediction method based on algorithms for climate change scenarios obtained from the Intergovernmental Panel on Climate Change. Salamanca et al. (2010) developed a new Building Energy Model (BEM) to further improve the heat transfer process in UCMs, including energy behaviors inside buildings and heat emissions from air conditioning systems. The Town Energy Balance (TEB) scheme was developed to simulate energy exchanges between a mesoscale atmospheric mode and urban surfaces covered by buildings, roads, or any artificial materials (Masson, 2000). Bueno, B et al. (2012) integrated BEM and TEB schemes, including passive building systems, in order to represent the impacts of building systems on urban climates and estimate large-scale building energy consumption. Recently, the Urban Weather Generator (UWG) was developed to calculate hourly air temperature and humidity in urban canyons from measured weather data outside of urban areas (Bueno et al., 2013b).

The UWG algorithm consists of four major models: 1) the Rural Station Model (RSM), 2) Vertical Diffusion Model (VDM), 3) Urban Boundary Layer Model (UBLM), and 4) Urban Canopy and Building Energy Model (UC-BEM). Figure 2 presents the conceptual calculation process of the UWG. Based on the measured weather data, the RSM calculates rural sensible heat fluxes (H_{rur}) that are delivered to the VDM and UBLM. The VDM produces vertical profiles of air temperatures (θ_{rur}) above the weather station using air temperatures (T_{rur}) and wind velocities from the weather data and sensible heat fluxes from the RSM; the air temperature profiles are provided to the UBLM. The UBLM then calculates the air temperatures (T_{ubl}) in the UBL, based on the temperature profiles (θ_{rur}) and two sets of sensible heat fluxes provided by the RSM and UC-BEM. The UC-BEM was developed based on the BEM-TEB scheme and energy conservation algorithms among different elements in urban canyons, in order to calculate air temperature (T_{ucl}) and humidity in the UCL. The calculation is conducted using the measured weather data, air temperature calculated from the UBL, and urban canyon energy balances such as the heat flux from walls, windows, and roads, waste heat from air conditioning, and anthropogenic heat sources (see Figure 2). The UWG assumes that air is well mixed in the UCL, meaning that each hour a single air temperature reading represents the urban air temperature in the UCL of a given UCM. It does not aim to simulate microclimatic conditions in the UCL. Various studies have been conducted to validate the reliability and robustness of the UWG in different cities such as Toulouse, France; Basel, Switzerland (Bueno et al., 2013a; Bueno et al.,

2013b); Singapore (Bueno et al., 2014); and Boston (Street et al., 2013). The detailed equations and models used in the UWG algorithm can be found in these studies.

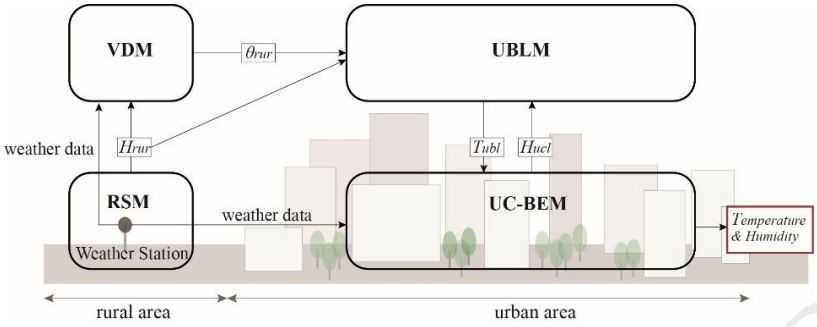

Figure 2. Conceptual calculation process of the UWG (Bueno et al., 2013b).

Envi-met, a three-dimensional non-hydrostatic model, was developed to simulate microscale surface-plant-air interactions among building envelopes, roofs, streets, vegetation, pavement, and greenery in urban areas; its outcome values include air temperature, mean radiant temperature, relative humidity, and global radiation (Bruse, 1998). Various empirical validation studies have been conducted that present the reliability of Envi-met by comparing it with field data in Guangzhou, South China (Yang et al., 2013); Bilbao, in the northern part of the Iberian Peninsula (Acero and Herranz-Pascual, 2015); and Rome, Italy (Salata et al., 2016). It has been used to investigate different issues related to sustainable urban environments including outdoor thermal comfort, building energy consumption, UHIs, and UHI mitigation strategies (Santamouris et al., 2018).

Computational Fluid Dynamics (CFD) and mesoscale atmospheric simulations have been implemented to predict urban weather and are used to investigate the impacts of urban climates on the energy consumption of buildings (Oxizidis et al., 2008). Yi and Malkawi (2012) integrated CFD simulations with Monte Carlo and artificial neural network simulations to reduce computational cost and the time taken to produce CFD simulations. The goal was to predict annual temperatures, wind speeds, and wind directions in urban areas. However, the CFD simulation process still has certain limitations when describing boundary conditions, due to a limited spatial scale, substantial simplification, and the extensive computing resources required (Erell and Williamson, 2006).

3.3 UHI Effect and Thermal Comfort Sensation

UHIs cause an increase in the risk of heat stress, a condition that is significantly related to human health (Tan et al., 2010) and life quality in cities (Chen and Ng, 2012). In built environments, the relative influence of UHIs on the level of heat stress depends on reginal climate conditions. In this regard, the evaluation of thermal comfort sensation at the pedestrian

level in the UCL should be investigated relative to the effects of UHIs. Saneinejad et al. (2014) investigated the impacts of three different UHI mitigation strategies on pedestrians' comfort level using the Universal Thermal Climate Index (UTCI), a widely used outdoor thermal comfort metric. The UTCI is the equivalent temperature of a reference environment that represents the same dynamic physiological response in the human body as in actual thermal conditions; the condition of the reference environment is described in Table 1. The UTCI can be calculated using a combination of wind, humidity, mean radiative temperature, and air temperature, and is categorized by a 10-level heat stress index ranging from extreme cold (below -40°C) to extreme heat stress (+46 °C) (Bröde et al., 2012). Although other thermal comfort indices such as physiological equivalent temperature have been used to measure thermal conditions, Blazejczyk et al. (2012) concluded that the UTCI is very sensitive to changes in meteorological values and is well-suited to representing bioclimatic conditions in a wide range of weather conditions.

Table 1. List of Metrological Input Values in the UTCI Reference Environment (Bröde et al., 2012)

Meteorological Input	**UTCI Reference Environment**
mean radiant temperature (Tr)	air temperature (Ta)
wind speed (va)	0.5 m/s (measured at 10m height)
relative humidity (rH)	50% (Ta < 29°C)
water vapour pressure (pa)	20 hPa (Ta > 29°C)
metabolic rate	walking 4 km/h (135 W/m2)

4 METHODOLOGY

In this research, a modeling and simulation approach was used to analyze the relative importance of UHI mitigation strategies in various climate zones in the United States. Based on UHI simulations and UTCI calculations, two case studies were conducted to represent the relative differences in UHIs effect. Figure 3 illustrates the overall workflow of the analysis, which consisted of three major steps: 1) creation of a base case UCM, 2) simulation of UHIs and calculation of the UTCI, and 3) evaluation and analysis of the results. The overall process of modeling and simulation was conducted based on a parametric modeling environment, Grasshopper, which is a graphical algorithm editor for the Rhinoceros 3D modeling tool (McNeel, 2010). Numerous studies have used parametric modeling technology for neighborhood -scale modeling and simulation research (Amado and Poggi, 2014; Taleb and Musleh, 2015; Yi and Kim, 2015, 2017). Detailed descriptions of the modeling and simulation process can be found in the following sections.

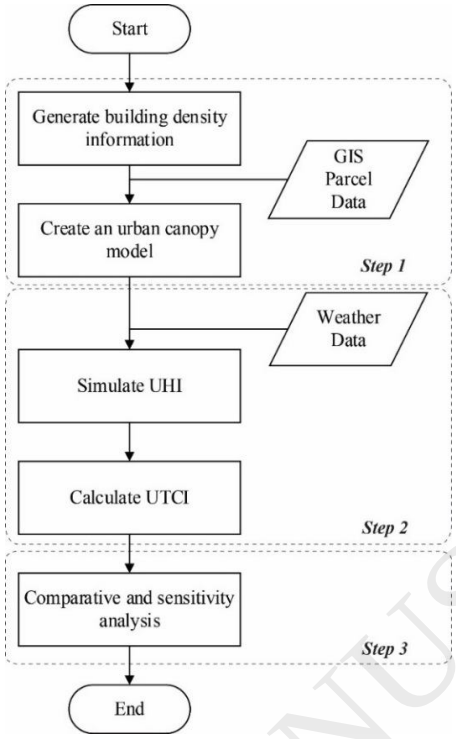

Figure 3. Overall workflow of the evaluation and analysis.

4.1 A Base Case UCM

As described in Figure 3, the first step was to create a base case UCM. We selected the downtown Houston area to serve as a representative high density, high-rise urban zone in the U.S., since the maximum UHI occurred in the densest part of the urban area (Giannopoulou et al., 2011). Houston is the fourth largest city in the U.S., and the downtown area includes various types of buildings, from skyscrapers to historic structures. Yu et al. (2010) estimated building density measurements using airborne LiDAR data for downtown Houston. This research divided the downtown Houston area into six urban districts according to distinct built environment settings, and measured each building's density attributes such as height, footprint, and volume. A base case UCM was developed based on the building density information they estimated and a set of urban block data from GIS, including street land-use from the Harris County Public GIS Database (Harris County Appraisal District, 2017). More precisely, the parcel data were imported into the parametric modeling environment, and then sorted to define the boundary of downtown Houston (as illustrated in Figure 4A). The model was made up of 280 blocks, organized in a grid pattern; the dimensions of each block were 86m × 86m (length × width) and the overall dimensions were 1360m × 1948m (length × width).

The 280 blocks were divided into five urban districts and two open space categories, including parks and parking spaces. The skyline district and sports and convention district were

located on the west and east sides, with 72 and 41 blocks, respectively. The theatre, historic, and other districts were located in the north and south areas, with 11, 32, and 42 blocks, respectively. The locations of the parking and green spaces were estimated based on the map included in Figure 4A and the GIS land-use data; they encompassed 57 and 27 blocks, respectively. The average building coverage ratio for each district was used to determine the building footprints, with an assumption that all buildings were rectangular. The height of each building was randomly generated to follow a normal distribution by giving the average height and its standard deviation for each district. For example, the average building coverage ratio, average building height, and standard deviation were 0.65, 118.5m, and 83.6m, respectively, in the skyline district of Houston; the detailed building density information can be found in the estimation conducted by Yu et al. (2010). Accordingly, the UCM represented a similar average building height and mass distribution to the existing building set in the downtown Houston area. In other words, the randomly assigned building heights mimicked the real built environment settings by district, while offering internal variations within each district. Figure 4B illustrates the base case UCM developed by following the above method.

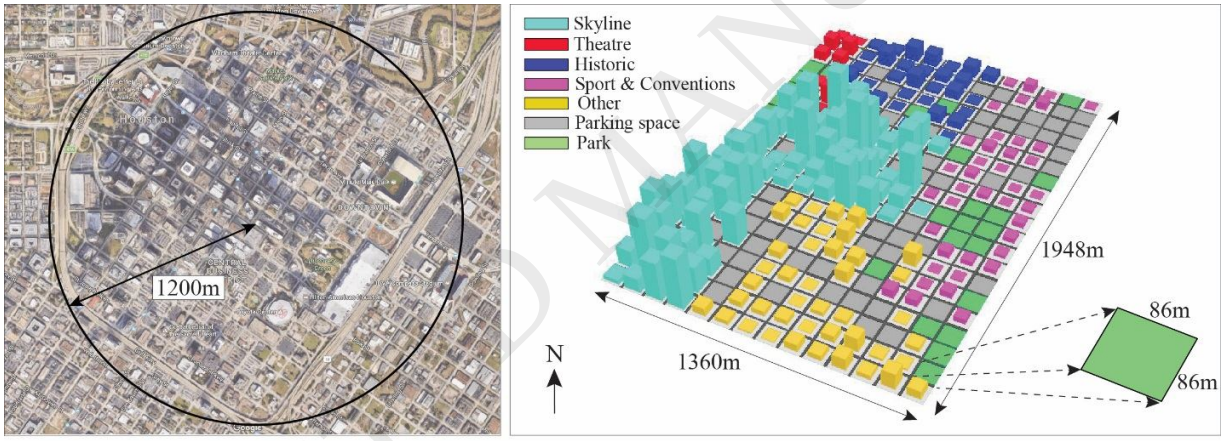

(A) Downtown Houston, TX (google map) (B) Urban Canopy Model (Downtown Houston, TX)

Figure 4. Base case urban canopy model.

4.2 Simulation of the UHI

In this research, the UWG algorithm was used to simulate the UHI effect. It was developed as a tool for the Rhinoceros modeling environment (Nakano et al., 2015; Norford and Reinhart, 2016). As a plug-in for Grasshopper, the tool was developed further to integrate parametric modeling and a UHI analysis program called Dragonfly (Mackey, 2017a), which was used in this research. Although UHI simulation requires a substantial number of parameters to represent a UCM, the user interface of the UWG categorizes key input parameters determined by a sensitivity analysis, including site coverage ratio, façade-to-site ratio, and sensible

anthropogenic heat (Nakano et al., 2015). Site coverage ratio is the ratio of the building footprint to the site area in the UCM; façade-to-site-ratio is the ratio of the area of the vertical wall to the urban plan area. Bueno et al. (2013b) called these terms horizontal building density and vertical-to-horizontal urban area ratio, respectively. For the base case UCM, the values of these two parameters were calculated based on the given urban geometry information. Stewart and Oke (2012) designed the Local Climate Zone (LCZ) classification system based on surface structure type, land cover, and human activities, in order to address various physical and climate characteristics. The sensible anthropogenic heat flux was set as 175 W/m^2 for the base case UCM, which was the average value of the compact high-rise LCZ (Stewart and Oke, 2012). Other parameters can be adjusted via the user interface. In terms of building type and construction parameters, the base case UCM used a set of constant values such as surface albedo; all buildings were assumed to be commercial, with an 80% window-wall ratio. The values of building construction, material, and internal loads were obtained from the U.S. Department of Energy (DOE) commercial reference building models of the national building stock, which complies with ANSI/ASHRAE/IES Standard 90.1-2010 (Deru et al., 2011). Other detailed input values of the base case UCM for the UWG simulation are described in Appendix 1.

In this study, three different parameters in the base case UCM were selected to conduct a comparative analysis. The UCM-related variables included roof vegetation, trees, and grass coverage ratio. The UWG user interface allowed for changes to be made to the ratio of roof vegetation and trees; the grass coverage ratios were calculated by manipulating the number of park blocks in the base case UCM. The UWG requires a weather dataset in an EnergyPlus Weather (EPW) file format and measured from a rural area, in order to morph a weather dataset (temperature and humidity) that includes the UHI effect in the UCM. The DOE provides standard climate zones for determination analyses. The entire United States is categorized into eight thermal zones; most are sub-divided into moist (A), dry (B), and marine (C) regions, representing a total of 15 climate zones (Halverson et al., 2014). In this study, six climate zones were selected as variables to investigate the relative impacts of climate characteristics on the UHI effect. A list of climate zones and their representative cities can be found in Table 2. This research used the Typical Meteorological Year (TMY3) weather data measured from a rural area near the city (the airport), representing long-term (30 years) weather conditions (Wilcox and Marion, 2008). For each city, average temperature and relative humidity during the hottest weeks in summer obtained from TMY3 weather data are described in Table 2. In terms of reference site input values in the UWG, the information obtained from the TMY3 weather data was used.

Table 2. Climate Zones and Representative Cites Used in this Study

Climate Zone	City	Hottest Week in Summer	Average Temperature and Relative Humidity
Hot and Humid	Houston, TX	July 29th to August 4th	29.7 °C / 70 %
Hot and Dry	Phoenix, AZ	August 3rd to August 9th	36.3 °C / 30 %
Warm and Humid	Memphis, TN	July 6th to July 12th	29.9 °C / 65 %
Warm and Dry	El Paso, TX	June 15th to June 21th	29.4 °C / 27%
Cool and Humid	Chicago, IL	July 20th to July 26th	27.1 °C / 65%
Cool and Dry	Boise, ID	August 3rd to August 9th	27.0 °C / 27%

5 COMPARATIVE AND SENSITIVITY ANALYSES OF MITIGATION STRATEGIES

The topics of inquiry driving this research included the following: 1) regional climate conditions' effects on the development of UHIs, and 2) current UHI mitigation strategies commonly incorporated into green building rating systems but not equally effective across different regional climates. Two case studies (one comparative and one sensitivity analysis) were conducted to address these issues.

5.1 Case Study 1

The UHI intensity is the temperature difference between the urban and rural areas. Previous studies have shown differences in UHI effect in different climates. For example, high UHI intensity levels were found in Phoenix (hot and dry); the average nighttime UHI intensity in summer is 5°C, and can increase up to 11°C (Hedquist and Brazel, 2014). In Chicago, the largest nighttime UHI intensity among eight different neighborhoods was 2.34°C in the summer of 2010 (Coseo and Larsen, 2014). According to records from Global Historical Climate Network data (2004-2013), the average minimum summer nighttime UHI intensities were 1.84°C, 1.89°C, 2.67°C, 3.11°C, and 3.77°C, in Houston, Chicago, Memphis, Boise, and Phoenix, respectively. The magnitudes of the UHI intensities varied across the entire U.S., based on regional and local characteristics (Kenward et al., 2014). In terms of weather conditions, higher UHI intensities occur in low wind speed and clear sky conditions (Santamouris, 2016), and low relative humidity (Gedzelman et al., 2003). Although previous studies have presented different magnitudes of UHIs for various cities, analysis outcomes have not been able to represent the impacts of climate conditions on UHIs, due to the measurements occurring in different urban settings.

To this extent, the first case study was conducted to investigate the relative impacts of six meteorological conditions on the UHI effect. The base case UCM and UWG input variables were used to estimate the UHI intensity. The analysis period was the hottest week of the typical mean year obtained from six different EPW files (see Table 2); this was selected to measure the temperature increase during the summer season. Figure 5 describes the average UHI intensities

obtained from the UWG simulations during the hottest weeks in six different climate conditions. Negative UHI intensities during the daytime were excluded from the representation of average UHI intensities. The results indicate that the UHI intensity differed significantly based on the climate conditions. Higher UHI intensities were measured in hot climates, as compared to warm and cool climates, except for in the case of Boise (cool and dry). The highest UHI intensity was measured in Boise (cool and dry), at 4.3°C (see Figure 5). A similar trend was found in actual measurements; the average summer nighttime UHI intensity in Boise ranked 13th among 60 cities in the U.S. (Kenward et al., 2014). It was relatively high considering the size of Boise, which is the 99th largest city in the U.S.

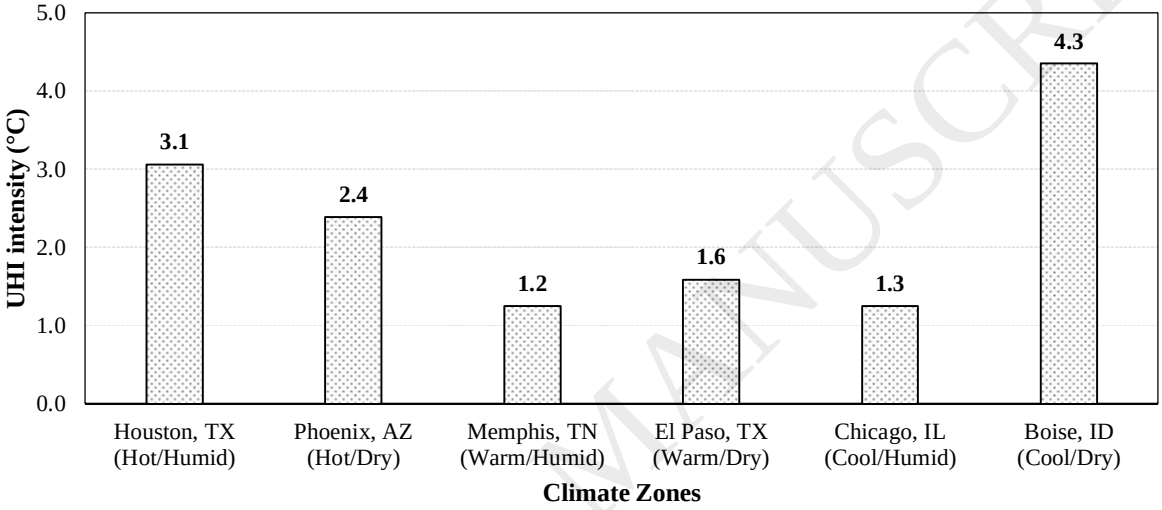

Figure 5. Average UHIs for the hottest weeks in different climate zones.

To increase the reliability of the UHI patterns, 20 different urban configuration scenarios were created by generating new random building height information for each block. In other words, 20 sets of building height data were used to produce different urban canopy models. Each followed a normal distribution of existing building characteristics to represent the existing urban morphology and UWG simulations, and each scenario was conducted independently. The average UHIs for the 20 scenarios and their 99% confidence intervals for the different climate zones are listed in Table 3. The range of the 99% confidence intervals for all six climate zones remained very close to the mean values, and each climate zone had non-overlapping confidence intervals. These results indicate that there were statistically significant differences between the mean UHIs at the 0.01 level of significance. In other words, each climate zone yielded unique UHIs with controlled urban built environments.

Table 3. Mean UHIs and 99% Confidence Intervals for Different Climate Zones

Climate	N	Mean	Standard	99% Confidence

			Error	Interval (CI)
Houston, TX (Hot/Humid)	20	3.059	0.0047	3.045 to 3.072
Phoenix, AZ (Hot/Dry)	20	2.384	0.0037	2.373 to 2.394
Memphis, TN (Warm/Humid)	20	1.246	0.0009	1.244 to 1.249
El Paso, TX (Warm/Dry)	20	1.587	0.0026	1.580 to 1.595
Chicago, IL (Cool/Humid)	20	1.253	0.0012	1.250 to 1.256
Boise, ID (Cool/Dry)	20	4.347	0.0009	4.344 to 4.350

The maximum UHI intensity during the hottest weeks is described in Table 4, along with the corresponding measured data and times. Although the maximum values showed a significant difference from the average values described in Figure 5, their rank order was the same. Figure 6 represents the hourly UHI intensity profiles in different climate zones for the days described in Table 4. Although there were differences in the degree of UHI intensity, in most cities, UHIs occurred after sunset and extended to sunrise (i.e., nighttime). The daytime UHI intensities were close to zero or negative values; this was the case everywhere except Chicago. This trend in summer UHI magnitude between daytime and nighttime was reinforced in numerous studies (Sailor, 2014). The positive daytime UHI intensity in Chicago (Coseo and Larsen, 2014) and negative intensity in Phoenix (Brazel et al., 2000) were especially common, as similar trends were seen in the outcomes of the UWG simulations (see Figure 6). The UHIs at night and during the day were relatively high and low in Boise and Memphis, respectively. However, this does not mean that Boise was the worst city in terms of thermal conditions during the summer season. The average urban temperatures for the days described in Table 4, in Boise and Memphis, were 27.9°C and 31.8°C, respectively, when the UHI effect occurred (see Figure 6). Conversely, Houston (hot and humid) and Phoenix (hot and dry) held the second and third ranks in the UHI effect list (see Figure 5). The highest daytime temperatures for these cities exceeded 40.0°C, due to the generally hot climatic conditions (see Figure 6). These results indicate that the UHI effect should be evaluated alongside an analysis of the surrounding climatic conditions.

Table 4. Maximum UHI Intensities and Corresponding Dates and Times

Cities	Maximum UHI Intensity (°C)	Date / Time
Houston, TX	9.3	August 5th (5am)
Phoenix, AZ	7	August 7th (7am)
Memphis, TN	3.2	July 9th (4am)
El Paso, TX	7	Jun 16th (3am)
Chicago, IL	5.7	July 25th (10am)
Boise, ID	10.6	August 8th (4am)

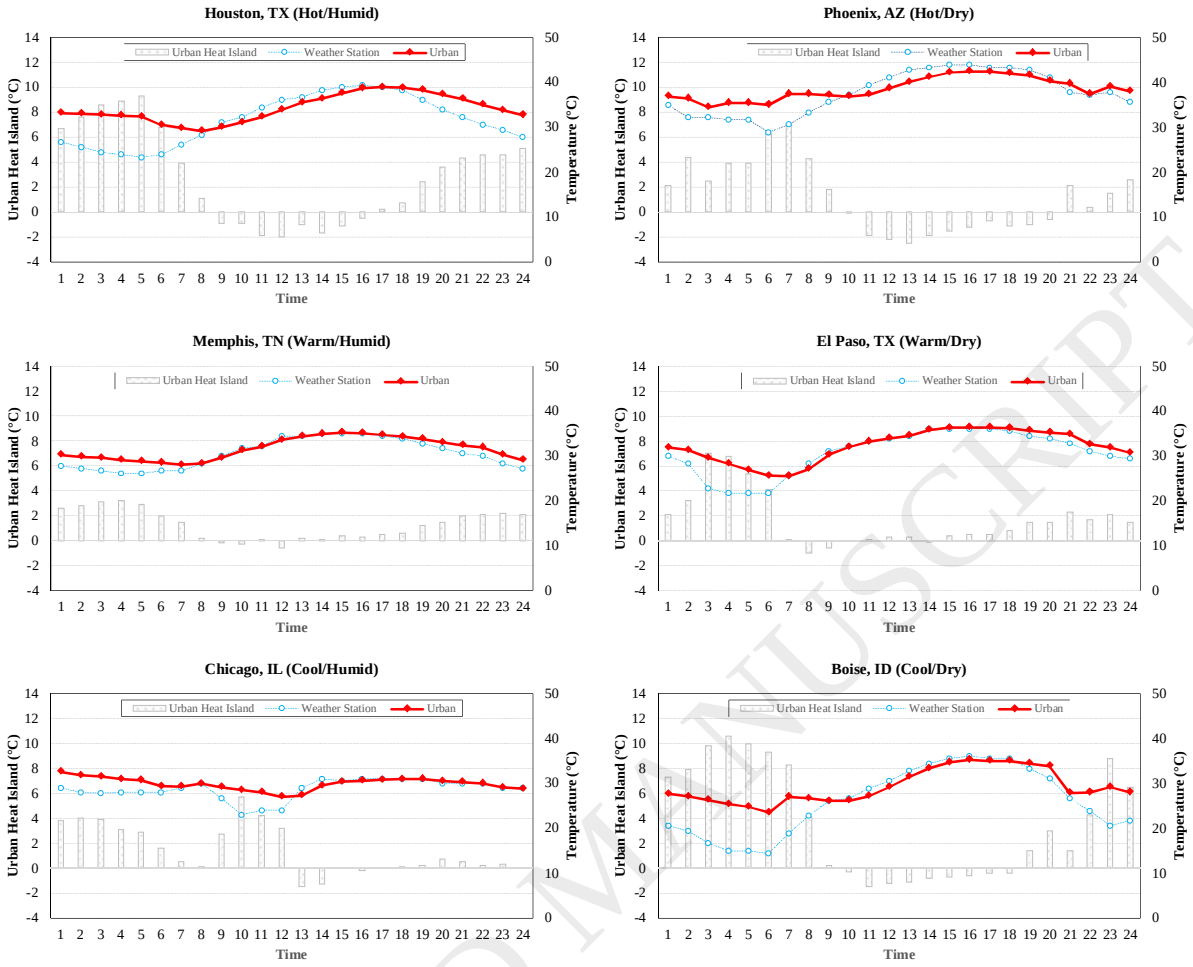

Figure 6. Hourly UHI intensity profiles for the maximum UHI values during the hottest weeks.

The level of heat stress was calculated based on the UTCI to investigate how much UHIs negatively affect urban areas. In this study, the UTCI was determined using the air temperature and relative humidity obtained from the UWG. Figure 7 shows the percentage of the UTCI that was above 28°C in each city's rural and urban areas during the hottest week. Moderate heat stress in the UTCI ranges from 26°C to 32°C. In most cases, the level of stress increases in urban areas, having negative impacts on public health, productivity, and energy savings. Rural climate conditions in Houston, Phoenix, and Memphis originally exhibited high levels of heat stress compared to other cities, due to a combination of high temperature and humidity. Boise showed the highest average UHI effect and lowest increase in heat stress (4.13%), meaning that the UHI effect was unlikely to be much of a problem compared to what was being experienced in other cities. Conversely, although relatively low UHI effects were measured in Memphis, El Paso, and Chicago, the condition could still pose an issue due to the high increase in heat stress: 8.94%,

7.16%, and 9.56%, respectively (see Figure 7). This means that climate conditions should be considered when prioritizing strategies for sustainable built environments.

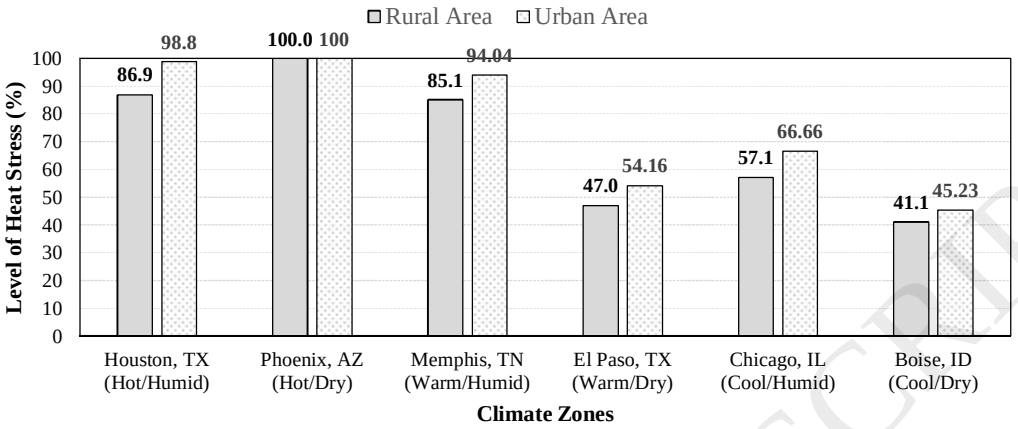

Figure 7. Percentage of the UTCI above 28°C during the hottest week.

5.2 Case Study 2

A sensitivity analysis was conducted to test the significance of UHI mitigation strategies in different climate conditions. The question pursued in Case Study 2 was if climatic conditions could affect the efficacy of UHI mitigation strategies. Green spaces covered by trees, shrubs, and grass (TSG); high albedo materials (HAM) for external building surfaces; and urban inland water bodies (UIWB) are known factors in UHI mitigation (O'Malley et al., 2015). In LEED v4, there are two main topics that address UHIs: 1) non-roof and roof, and 2) parking under cover. These include guidelines for minimizing hardscape (paved roads, sidewalks, courtyards, and parking lots), and identifying materials (roof and non-roof) and shaded areas (trees and parking under cover) (USGBC). Material properties significantly affect UHIs by rejecting solar heat, which can be measured as an SRI value. However, this research did not address the issue of SRI values in UHI mitigation strategies.

Instead, UHI mitigation strategies (such as roof vegetation, trees, and grass coverage ratio) were the parameters employed to judge the sensitivity of the UHI mitigation effect. Installing green roofs, planting trees, and incorporating vegetation are common means of modifying the urban climate and resultant impact on building energy performance (Davies et al., 2008). Table 5 lists the test cases for the sensitivity analysis. In the base case UCM, 1% of the roof area of the entire building was assumed to be covered with vegetation. The ratio was increased at 10% intervals for all buildings' roofs in Cases 1 to 5. The initial tree coverage was 10% of the urban area. From Case 1 to Case 5, the ratio increased from 20% to 60%. The grass coverage ratio in

the base case UCM was 7.5% of the entire area. It was increased by changing the parking blocks in the base case UCM to green parking spaces at 20% intervals. For example, the total number of grass lots (parks) and parking blocks were 27 and 57, respectively, in the base case UCM. In Case 1, 20% of the parking block was changed to grass parking spaces. The maximum grass coverage ratio for the entire block was 23% of the entire area in Case 5.

Table 5. UWG Input Variables Used for the Sensitivity Analysis

Input Variables	**Base Case**	**Case 1**	**Case 2**	**Case 3**	**Case 4**	**Case 5**
Roof vegetation coverage ratio	0.01	0.1	0.2	0.3	0.4	0.5
Tree coverage ratio	0.1	0.2	0.3	0.4	0.5	0.6
Grass coverage ratio	0.075	0.1	0.14	0.17	0.20	0.23

Figure 8 shows the impacts of the three parameters on the UHI effects in different climate zones using the base case UCM. It illustrates the average UHI intensity with the three mitigation strategies during the same simulation period as Case Study 1. Mostly, it includes the nighttime UHIs, except for those from Chicago. Overall, an increase in the roof vegetation coverage ratio had very little effect on UHI mitigation in all climate zones. Green roofs decrease the surface temperature and the amount of sensible heat released from the roof. Additional benefits are related to energy savings, noise reduction, and air quality (Santamouris, 2015). In terms of sensible heat reduction from green roofs on a mesoscale, impact on UHI mitigation was found in low-rise buildings. There was no significant heat mitigation from green roofs in high and mid-rise urban areas (Santamouris, 2015). A large portion of the base case UCM used in this study was comprised of high-rise buildings with an average height of 118.5m. Thus, green roofs might have a slight effect on UHIs in these urban canyons. The additional green spaces, including parks and trees in urban areas, significantly contributed to reducing the UHI effect by offering shade and encouraging an evaporation cooling effect during the daytime. High radiative cooling and decreased convective release were key cooling processes during the nighttime, especially on cloudless nights (Santamouris, 2015). The increase in grass coverage ratio was effective in hot climates in Houston and Phoenix, but only slightly effective in Memphis and resulting in an increase in the UHI effect in the other climate zones. Tree coverage ratio was an effective strategy for mitigating UHIs in most of the test case climate zones, especially in Houston (hot and humid) and Memphis (warm and humid). The sensitivity analysis conducted for this research

showed that UHI mitigation strategies should be differently employed based on the particular climate conditions and UCMs. This means that green building rating systems must update their rating criteria, including the characteristics of the UCM and climate conditions, in order to obtain more effective benefits. For example, in high-rise cities in hot climate zones, an increase in green parking lots with trees should be more of a priority than the installation of green roofs, at least with regards to UHI mitigation.

The estimated sensitivities of the UHI effect by climate condition help to illustrate the efficiency levels of various UHI mitigation strategies. In addition, the estimated temperature mitigation results suggest tailored values for each strategy in each climate zone, allowing for the best use of vegetated spaces in urban areas. In the case of Chicago, all strategies were ineffective or had a negative influence on the UHI; this unique characteristic was also found in Case Study 1 in that the highest UHI intensity occurred during the daytime. This might have originated from the high cloud coverage ratio during the hottest week in Chicago, which was an average of 59% during the week. This was relatively higher than in the other five cities, which showed an approximate average of 20%~40%. Additional tests during other periods in Chicago and cities in cool and humid climates are necessary to properly investigate the trend of effectiveness of mitigation strategies. Although the results of the Chicago case seem to be unique, they may also indicate the need for a climate-based application of UHI mitigation strategies.

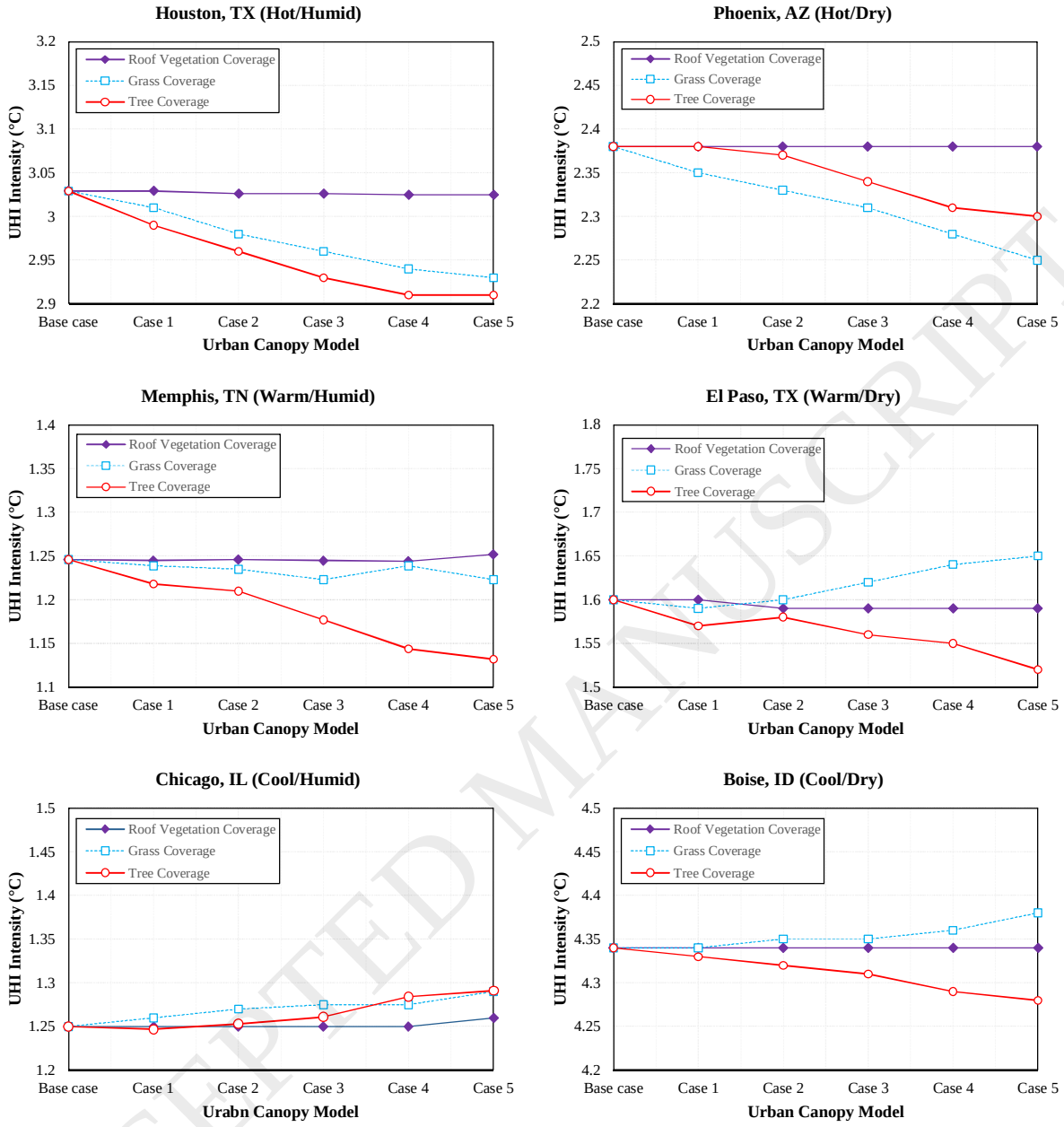

Figure 8. Average UHI intensity from various green coverage ratios in different climate zones.

6 DISCUSSION

In this study, the base case UCM represented a high density high-rise urban morphology, and the analyses of UWG simulations were conducted during the hottest weeks in six cities selected to represent difference climate conditions. It is import to note that the scope and limitations of this research are as follows:

- Although the authors tested different urban configurations, all cases represented high-rise urban environments. Mid- and low-rise urban configurations still need to be tested in various climate conditions, along with the accompanying UHI mitigation strategies. The effectiveness of green roofs, especially, should be considered, along with the characteristics of the particular urban morphology. Vegetated roofs, trees, and the grass coverage ratio all depend on the urban morphology, and their respective impacts might differ when different urban district information is used.
- Climate conditions include several factors such as wind speed, humidity, precipitation, and clouds. All play a significant role in the development of UHIs. In this study, the impacts of each factor on UHIs were not considered in the analysis. Thus, different cities in the same climate zone might have different UHI potentials and behaviors, based on the climate factors. More test cases with different cities in each climate zone are required to properly investigate the impact of climate conditions.
- The UWG simulations produced mesoscale UHIs, following the assumption that air in the UCL was well-mixed. The integration of microscale UHIs and thermal comfort simulations are necessary to increase the reliability of the analysis outcomes.
- Although green building rating systems include several factors associated material properties, this study was limited to green coverage ratios. Testing according to a rating system with more detailed criteria, including material properties, is needed to establish a climate-based priority in the rating system.
- It should be noted that the built environment conditions we used for the UWG simulations were comprised of a simplified model that was based on the Houston downtown area. This served as a general proxy for urban downtown areas in the U.S., and accordingly did not offer an affirmative answer regarding how a built environment might itself affect UHIs.
- More than 100 thermal indices have been developed to address human bioclimatic conditions and indoor and outdoor temperatures (Blazejczyk et al., 2012; De Dear et al., 1998). While the latest UTCI model, UTCI-Fiala, offers the human behavioral adaptation of clothing based on the bioheat transfer equation (Fiala et al., 2012), there are other factors not addressed in the model, such as human preferences according to preexisting climate conditions. For example, people living in a warm climate zone might prefer warmer temperatures than people living in a cold climate zone (De Dear et al., 1998). Accordingly, the illustrated UHIs and following UTCI results were not able to consider the physiological adaptation of residents in each city.

7 CONCLUSION

This research presents the effect of climate conditions on UHIs, and the various efficacy levels of UHI mitigation strategizes in a controlled urban setting. A high density high-rise UCM was developed using statistical urban and building information to replicate an existing urban morphology. The simulated UHI effects show that climate conditions have a substantial influence on both the UHI effect itself and the efficiency levels of various UHI mitigation strategies. From the analysis results of Case Study 1, it can be seen that the confidence intervals of the UHI effects in each climate zone did not overlap, indicating statistically significant temperature differences due to disparate climate conditions. In addition, the results from Case Study 2 show that the UHI mitigation effects from increased green coverage ratios on parking lot surfaces with planted trees were affected by climate conditions. These results imply that we may question the effectiveness of a "one-size-fits-all" UHI mitigation strategy of planting trees and vegetation on any available urban surface, regardless of regional climate.

In summary, the simulated results indicate that estimations of UHI effects and measurements of efficiency levels of UHI mitigation strategies should consider climate conditions in order to develop sustainable built environments. Although more sophisticated built environment input factors should be introduced in future research, the results of this research lead us to conclude that an overall focus on climate conditions is a vital aspect of estimating and mitigating the UHI effect. Moreover, an urban development direction should be customized to local climate conditions to build sustainable cities. This adaptation requires physical modifications to buildings and their surroundings, and thus demands long-term planning at the city and district levels (Smid and Costa, 2017). To this extent, the suggested simulation method enables the incorporation of design guidelines such as building height, floor area ratio, and setback regulations when investigating the expected UHI effects during the early design stage of urban development.

Appendix

Appendix 1 Input Values in the Base Case UCM for the UWG Simulation

Category	UWG Input Parameter			Input value
Building Typology	Construction[1]	Wall	Albedo	0.4
			Emissivity	0.9
			Vegetation coverage ratio	0.001
		Roof	Albedo	0.2
			Emissivity	0.9
			Vegetation coverage ratio[2]	0.01
		Window	Window-wall ratio[3]	0.8
	Building parameters[4]	Daytime internal heat gain (W/m^2)		16.69
		Nighttime internal heat gain (W/m^2)		4.73
		Infiltration (ACH)[5]		0.16
		Ventilation (ACH)[5]		0.41
		Nighttime cooling set point (°C)		24.4
		Daytime cooling set point (°C)		26.0
Urban Area	Urban road	Albedo[6]		0.165
		Thermal conductivity ($W/(m \cdot K)$)[7]		1
		Volumetric heat capacity (J/m^3K)[7]		1,600,000
	Average building height (m)[8]			78.8
	Site coverage ratio[8]			0.29
	Façade-to-site ratio[8]			1.40
	Tree coverage ratio[2]			1.5
	Sensible anthropogenic heat flux (W/m^2)[9]			157.5
	Latent anthropogenic heat (W/m^2)[9]			17.5
	Latent fraction of trees[7]			0.7
	Latent fraction of grass[7]			0.6
	Vegetation albedo[10]			0.25
Boundary Layer	Daytime boundary-layer height (m)[6]			700
	Nighttime boundary-layer height (m)[6]			80
	Reference height (m)[6]			150

Notes:

1. For each city, different building construction parameters such as material properties and U-value (window) were assigned based on the climate zones of the EPW weather files and ASHRAE reference building models (Deru et al., 2011).

2. These variables were used for the sensitivity analysis in Case Study 2 (see Table 5).

3. An 80% window-wall ratio was assigned regardless of climate zone.

4. We assumed all test cases included the same building parameter values (Deru et al., 2011).

5. Air Changes per Hour (ACH)

6. The value was estimated based on the range of surface albedos of LCZ built types (1 to 6) (Stewart and Oke, 2012).

7. These values were estimated from previous studies (Bueno et al., 2014).

8. The input values were calculated based on the base case UCM (see Figure 4) (Harris County Appraisal District, 2017; Yu et al., 2010).

9. The heat originated from fuel combustion and human activity (transportation, space cooling/heating, industrial processing, and human metabolism), except buildings. We used the average value of a compact high-rise LCZ (Stewart and Oke, 2012) and assumed that the latent anthropogenic heat was 10% of the anthropogenic sensible heat.

10. The value was estimated based on the range of surface albedos of LCZ land cover types (A to E) (Stewart and Oke, 2012).

* In this study, an input file for the UWG simulation was created by modifying an example file developed by Mackey (2017b).

ACKNOWLEDGMENTS

This work was supported by Incheon National University Research Grant in 2015. The authors would like to express our appreciation for the generous help received from the university.

REFERENCES

Acero, J.A., Herranz-Pascual, K., 2015. A comparison of thermal comfort conditions in four urban spaces by means of measurements and modelling techniques. Building and Environment 93, 245-257.
Akbari, H., 2002. Shade trees reduce building energy use and CO2 emissions from power plants. Environmental Pollution 116, S119-S126.
Akbari, H., Pomerantz, M., Taha, H., 2001. Cool surfaces and shade trees to reduce energy use and improve air quality in urban areas. Solar Energy 70(3), 295-310.
Alexandri, E., Jones, P., 2008. Temperature decreases in an urban canyon due to green walls and green roofs in diverse climates. Building and Environment 43(4), 480-493.
Amado, M., Poggi, F., 2014. Solar urban planning: A parametric approach. Energy Procedia 48, 1539-1548.
Arnfield, A.J., 2003. Two decades of urban climate research: a review of turbulence, exchanges of energy and water, and the urban heat island. International journal of climatology 23(1), 1-26.
Asaeda, T., Ca, V.T., Wake, A., 1996. Heat storage of pavement and its effect on the lower atmosphere. Atmospheric Environment 30(3), 413-427.
Blazejczyk, K., Epstein, Y., Jendritzky, G., Staiger, H., Tinz, B., 2012. Comparison of UTCI to selected thermal indices. International journal of biometeorology 56(3), 515-535.
Bourdic, L., Salat, S., 2012. Building energy models and assessment systems at the district and city scales: a review. Building Research & Information 40(4), 518-526.
Brazel, A., Selover, N., Vose, R., Heisler, G., 2000. The tale of two climates—Baltimore and Phoenix urban LTER sites. Climate Research 15(2), 123-135.
Bröde, P., Fiala, D., Błażejczyk, K., Holmér, I., Jendritzky, G., Kampmann, B., Tinz, B., Havenith, G., 2012. Deriving the operational procedure for the Universal Thermal Climate Index (UTCI). International journal of biometeorology 56(3), 481-494.
Brown, M.J., Grimmond, S., Ratti, C., 2001. COMPARISON OF METHODOLOGIES FOR COMPUTING SKY VIEW FACTOR IN URBAN ENVIRONMENTS. ; Los Alamos National Lab., NM (US).
Bruse, M., 1998. Simulating surface-plant-air interactions inside urban environments with a three dimensional numerical model. Environmental modelling & software 13(3/4), 373-384.
Bueno, B., Hidalgo, J., Pigeon, G., Norford, L., Masson, V., 2013a. Calculation of air temperatures above the urban canopy layer from measurements at a rural operational weather station. Journal of Applied Meteorology and Climatology 52(2), 472-483.
Bueno, B., Norford, L., Hidalgo, J., Pigeon, G., 2013b. The urban weather generator. Journal of Building Performance Simulation 6(4), 269-281.
Bueno, B., Norford, L., Pigeon, G., Britter, R., 2012. A resistance-capacitance network model for the analysis of the interactions between the energy performance of buildings and the urban climate. Building and Environment 54, 116-125.
Bueno, B., Pigeon, G., Norford, L., Zibouche, K., Marchadier, C., 2012. Development and evaluation of a building energy model integrated in the TEB scheme.
Bueno, B., Roth, M., Norford, L., Li, R., 2014. Computationally efficient prediction of canopy level urban air temperature at the neighbourhood scale. Urban Climate 9, 35-53.
Busato, F., Lazzarin, R.M., Noro, M., 2014. Three years of study of the Urban Heat Island in Padua: Experimental results. Sustainable Cities and Society 10(Supplement C), 251-258.

Chen, H., Ooka, R., Huang, H., Tsuchiya, T., 2009. Study on mitigation measures for outdoor thermal environment on present urban blocks in Tokyo using coupled simulation. Building and Environment 44(11), 2290-2299.
Chen, L., Ng, E., 2012. Outdoor thermal comfort and outdoor activities: A review of research in the past decade. Cities 29(2), 118-125.
Chen, L., Ng, E., An, X., Ren, C., Lee, M., Wang, U., He, Z., 2012. Sky view factor analysis of street canyons and its implications for daytime intra-urban air temperature differentials in high-rise, high-density urban areas of Hong Kong: a GIS-based simulation approach. International journal of climatology 32(1), 121-136.
Coseo, P., Larsen, L., 2014. How factors of land use/land cover, building configuration, and adjacent heat sources and sinks explain Urban Heat Islands in Chicago. Landscape and Urban Planning 125, 117-129.
Crawley, D.B., 2008. Estimating the impacts of climate change and urbanization on building performance. Journal of Building Performance Simulation 1(2), 91-115.
Davies, M., Steadman, P., Oreszczyn, T., 2008. Strategies for the modification of the urban climate and the consequent impact on building energy use. Energy Policy 36(12), 4548-4551.
De Dear, R.J., Brager, G.S., Reardon, J., Nicol, F., 1998. Developing an adaptive model of thermal comfort and preference/discussion. ASHRAE transactions 104, 145.
Debbage, N., Shepherd, J.M., 2015. The urban heat island effect and city contiguity. Computers, Environment and Urban Systems 54, 181-194.
Deru, M., Field, K., Studer, D., Benne, K., Griffith, B., Torcellini, P., Liu, B., Halverson, M., Winiarski, D., Rosenberg, M., Yazdanian, M., Huang, J., Crawley, D., 2011. US Department of Energy commercial reference building models of the national building stock. pp. 1-118.
Dimoudi, A., Zoras, S., Kantzioura, A., Stogiannou, X., Kosmopoulos, P., Pallas, C., 2014. Use of cool materials and other bioclimatic interventions in outdoor places in order to mitigate the urban heat island in a medium size city in Greece. Sustainable Cities and Society 13(Supplement C), 89-96.
Du, H., Wang, D., Wang, Y., Zhao, X., Qin, F., Jiang, H., Cai, Y., 2016. Influences of land cover types, meteorological conditions, anthropogenic heat and urban area on surface urban heat island in the Yangtze River Delta Urban Agglomeration. Science of the Total Environment 571, 461-470.
Environmental Protection Agency, 2017. Heat Island Effect. https://www.epa.gov/heat-islands. (Accessed November 26 2017 2017).
Erell, E., Williamson, T., 2006. Simulating air temperature in an urban street canyon in all weather conditions using measured data at a reference meteorological station. International Journal of Climatology 26(12), 1671-1694.
Eto, J.H., 1988. On using degree-days to account for the effects of weather on annual energy use in office buildings. Energy and Buildings 12(2), 113-127.
Fiala, D., Havenith, G., Bröde, P., Kampmann, B., Jendritzky, G., 2012. UTCI-Fiala multi-node model of human heat transfer and temperature regulation. International Journal of Biometeorology 56(3), 429-441.
Gál, T., Lindberg, F., Unger, J., 2009. Computing continuous sky view factors using 3D urban raster and vector databases: comparison and application to urban climate. Theoretical and applied climatology 95(1-2), 111-123.

Gedzelman, S., Austin, S., Cermak, R., Stefano, N., Partridge, S., Quesenberry, S., Robinson, D., 2003. Mesoscale aspects of the urban heat island around New York City. Theoretical and Applied Climatology 75(1-2), 29-42.
Georgescu, M., 2015. Challenges associated with adaptation to future urban expansion. Journal of Climate 28(7), 2544-2563.
Georgescu, M., Morefield, P.E., Bierwagen, B.G., Weaver, C.P., 2014. Urban adaptation can roll back warming of emerging megapolitan regions. Proceedings of the National Academy of Sciences 111(8), 2909-2914.
Giannopoulou, K., Livada, I., Santamouris, M., Saliari, M., Assimakopoulos, M., Caouris, Y.G., 2011. On the characteristics of the summer urban heat island in Athens, Greece. Sustainable Cities and Society 1(1), 16-28.
Gu, D., Kim, H., Kim, H., 2015. LEED, its efficacy in regional context: Finding a relationship between regional measurements and urban temperature. Energy and Buildings 86(Supplement C), 687-691.
Halverson, M.A., Rosenberg, M.I., Hart, P.R., Richman, E.E., Athalye, R.A., Winiarski, D.W., 2014. ANSI/ASHRAE/IES Standard 90.1-2013 Determination of Energy Savings: Qualitative Analysis. Pacific Northwest National Laboratory (PNNL), Richland, WA (US).
Han, S.-G., Huh, J.-H., 2008. Estimate of the heat island and building cooling load changes due to the restored stream in Seoul, Korea. International Journal of Urban Sciences 12(2), 129-145.
Harlan, S.L., Ruddell, D.M., 2011. Climate change and health in cities: impacts of heat and air pollution and potential co-benefits from mitigation and adaptation. Current Opinion in Environmental Sustainability 3(3), 126-134.
Harris County Appraisal District, 2017. HCAD Public Data. http://pdata.hcad.org/. (Accessed October 02 2017).
Hassid, S., Santamouris, M., Papanikolaou, N., Linardi, A., Klitsikas, N., Georgakis, C., Assimakopoulos, D., 2000. The effect of the Athens heat island on air conditioning load. Energy and Buildings 32(2), 131-141.
Hathway, E.A., Sharples, S., 2012. The interaction of rivers and urban form in mitigating the Urban Heat Island effect: A UK case study. Building and Environment 58(Supplement C), 14-22.
He, J., Hoyano, A., 2010. Experimental study of cooling effects of a passive evaporative cooling wall constructed of porous ceramics with high water soaking-up ability. Building and Environment 45(2), 461-472.
Hedquist, B.C., Brazel, A.J., 2014. Seasonal variability of temperatures and outdoor human comfort in Phoenix, Arizona, USA. Building and Environment 72, 377-388.
Heidt, V., Neef, M., 2008. Benefits of urban green space for improving urban climate, Ecology, Planning, and Management of Urban Forests. Springer, pp. 84-96.
Horvat, M., Fazio, P., 2005. Comparative review of existing certification programs and performance assessment tools for residential buildings. Architectural science review 48(1), 69-80.
Jansson, Å., 2013. Reaching for a sustainable, resilient urban future using the lens of ecosystem services. Ecological Economics 86(Supplement C), 285-291.
Karl, T.R., Diaz, H.F., Kukla, G., 1988. Urbanization: Its detection and effect in the United States climate record. Journal of Climate 1(11), 1099-1123.
Kennedy, C., Steinberger, J., Gasson, B., Hansen, Y., Hillman, T., Havranek, M., Pataki, D., Phdungsilp, A., Ramaswami, A., Mendez, G.V., 2009. Greenhouse gas emissions from global cities. Environmental Science & Technology 43(19), 7297-7302.

Kenward, A., Yawitz, D., Sanford, T., Wang, R., 2014. Summer in the city: hot and getting hotter. Clim Cent, Princeton, 1-29.
Kleerekoper, L., van Esch, M., Salcedo, T.B., 2012. How to make a city climate-proof, addressing the urban heat island effect. Resources, Conservation and Recycling 64(Supplement C), 30-38.
Kolokotroni, M., Ren, X., Davies, M., Mavrogianni, A., 2012. London's urban heat island: Impact on current and future energy consumption in office buildings. Energy and Buildings 47(Supplement C), 302-311.
Krüger, E.L., Pearlmutter, D., 2008. The effect of urban evaporation on building energy demand in an arid environment. Energy and Buildings 40(11), 2090-2098.
Kuttler, W., 2008. The urban climate–basic and applied aspects, Urban ecology. Springer, pp. 233-248.
Layberry, R., 2008. Degree days for building energy management—presentation of a new data set. Building Services Engineering Research and Technology 29(3), 273-282.
Liu, K., 2002. Energy efficiency and environmental benefits of rooftop gardens. Construction Canada 44(2), 17-23.
Machairas, V., Tsangrassoulis, A., Axarli, K., 2014. Algorithms for optimization of building design: A review. Renewable and Sustainable Energy Reviews 31, 101-112.
Mackey, C., 2017a. Dragonfly: A Plugin for Climate Data Generation. Available at: https://github.com/chriswmackey/Dragonfly.
Mackey, C., 2017b. Urban Weather Generator Workflow. Available at: http://hydrashare.github.io/hydra/viewer?owner=chriswmackey&fork=hydra_2&id=Urban_Weather_Generator_Workflow&slide=0&scale=1&offset=0,0.
Masson, V., 2000. A physically-based scheme for the urban energy budget in atmospheric models. Boundary-layer meteorology 94(3), 357-397.
Mavrogianni, A., Davies, M., Batty, M., Belcher, S.E., Bohnenstengel, S.I., Carruthers, D., Chalabi, Z., Croxford, B., Demanuele, C., Evans, S., Giridharan, R., Hacker, J.N., Hamilton, I., Hogg, C., Hunt, J., Kolokotroni, M., Martin, C., Milner, J., Rajapaksha, I., Ridley, I., Steadman, J.P., Stocker, J., Wilkinson, P., Ye, Z., 2011. The comfort, energy and health implications of London's urban heat island. Building Services Engineering Research and Technology 32(1), 35-52.
McNeel, R., 2010. Grasshopper generative modeling for Rhino. Computer software (2011b). <http://www.grasshopper3d.com/>. (accessed 15 March 2016).
Mohareb, E.A., Kennedy, C.A., Harvey, L.D.D., Pressnail, K.D., 2011. Decoupling of building energy use and climate. Energy and Buildings 43(10), 2961-2963.
Nakano, A., Bueno, B., Norford, L., Reinhart, C.F., 2015. Urban Weather Generator-a Novel Workflow for Integrating Urban Heat Island Effect within Urban Design Process, 14th International Conference of IBPSA: Building Simulation 2015 (BS2015). IBPSA, Hyderabad, India.
Nakayama, T., Fujita, T., 2010. Cooling effect of water-holding pavements made of new materials on water and heat budgets in urban areas. Landscape and Urban Planning 96(2), 57-67.
Newsham, G.R., Mancini, S., Birt, B.J., 2009. Do LEED-certified buildings save energy? Yes, but…. Energy and Buildings 41(8), 897-905.
Norford, L., Reinhart, C., 2016. Urban Weather Generator. Computer software. <http://urbanmicroclimate.scripts.mit.edu/uwg.php>. (accessed 15 May 2018).

O'Malley, C., Piroozfar, P., Farr, E.R., Pomponi, F., 2015. Urban Heat Island (UHI) mitigating strategies: A case-based comparative analysis. Sustainable Cities and Society 19, 222-235.
Oke, T., Johnson, G., Steyn, D., Watson, I., 1991. Simulation of surface urban heat islands under 'ideal'conditions at night Part 2: Diagnosis of causation. Boundary-Layer Meteorology 56(4), 339-358.
Oke, T.R., 1981. Canyon geometry and the nocturnal urban heat island: Comparison of scale model and field observations. Journal of climatology 1(3), 237-254.
Oke, T.R., 1982. The energetic basis of the urban heat island. Quarterly Journal of the Royal Meteorological Society 108(455), 1-24.
Oxizidis, S., Dudek, A., Papadopoulos, A., 2008. A computational method to assess the impact of urban climate on buildings using modeled climatic data. Energy and Buildings 40(3), 215-223.
Ramamurthy, P., Bou-Zeid, E., 2017. Heatwaves and urban heat islands: A comparative analysis of multiple cities. Journal of Geophysical Research: Atmospheres 122(1), 168-178.
Rosenfeld, A.H., Akbari, H., Romm, J.J., Pomerantz, M., 1998. Cool communities: strategies for heat island mitigation and smog reduction. Energy and Buildings 28(1), 51-62.
Runsheng, T., Etzion, Y., Erell, E., 2003. Experimental studies on a novel roof pond configuration for the cooling of buildings. Renewable Energy 28(10), 1513-1522.
Rydin, Y., Bleahu, A., Davies, M., Dávila, J.D., Friel, S., De Grandis, G., Groce, N., Hallal, P.C., Hamilton, I., Howden-Chapman, P., Lai, K.-M., Lim, C.J., Martins, J., Osrin, D., Ridley, I., Scott, I., Taylor, M., Wilkinson, P., Wilson, J., 2012. Shaping cities for health: complexity and the planning of urban environments in the 21st century. Lancet 379(9831), 2079-2108.
Sailor, D.J., 2014. Risks of summertime extreme thermal conditions in buildings as a result of climate change and exacerbation of urban heat islands. Building and Environment 78, 81-88.
Sailor, D.J., Lu, L., 2004. A top–down methodology for developing diurnal and seasonal anthropogenic heating profiles for urban areas. Atmospheric environment 38(17), 2737-2748.
Salamanca, F., Krpo, A., Martilli, A., Clappier, A., 2010. A new building energy model coupled with an urban canopy parameterization for urban climate simulations—part I. formulation, verification, and sensitivity analysis of the model. Theoretical and applied climatology 99(3-4), 331.
Salata, F., Golasi, I., de Lieto Vollaro, R., de Lieto Vollaro, A., 2016. Urban microclimate and outdoor thermal comfort. A proper procedure to fit ENVI-met simulation outputs to experimental data. Sustainable Cities and Society 26, 318-343.
Saneinejad, S., Moonen, P., Carmeliet, J., 2014. Comparative assessment of various heat island mitigation measures. Building and environment 73, 162-170.
Saneinejad, S., Moonen, P., Defraeye, T., Carmeliet, J., 2011. Analysis of convective heat and mass transfer at the vertical walls of a street canyon. Journal of Wind Engineering and Industrial Aerodynamics 99(4), 424-433.
Saneinejad, S., Moonen, P., Defraeye, T., Derome, D., Carmeliet, J., 2012. Coupled CFD, radiation and porous media transport model for evaluating evaporative cooling in an urban environment. Journal of Wind Engineering and Industrial Aerodynamics 104-106, 455-463.
Santamouris, M., 2013. On the built environment—the urban influence. Energy and Climate in the Urban Built Environment, 3-18.
Santamouris, M., 2014a. Cooling the cities – A review of reflective and green roof mitigation technologies to fight heat island and improve comfort in urban environments. Solar Energy 103(Supplement C), 682-703.

Santamouris, M., 2014b. On the energy impact of urban heat island and global warming on buildings. Energy and Buildings 82(Supplement C), 100-113.
Santamouris, M., 2015. Regulating the damaged thermostat of the cities—Status, impacts and mitigation challenges. Energy and Buildings 91, 43-56.
Santamouris, M., 2016. URBAN WARMING AND MITIGATION.
Santamouris, M., Haddad, S., Saliari, M., Vasilakopoulou, K., Synnefa, A., Paolini, R., Ulpiani, G., Garshasbi, S., Fiorito, F., 2018. On the energy impact of urban heat island in Sydney: Climate and energy potential of mitigation technologies. Energy and Buildings 166, 154-164.
Santamouris, M., Papanikolaou, N., Livada, I., Koronakis, I., Georgakis, C., Argiriou, A., Assimakopoulos, D., 2001. On the impact of urban climate on the energy consumption of buildings. Solar energy 70(3), 201-216.
Santamouris, M., Synnefa, A., Karlessi, T., 2011. Using advanced cool materials in the urban built environment to mitigate heat islands and improve thermal comfort conditions. Solar Energy 85(12), 3085-3102.
Shin, M.H., Kim, H.Y., Gu, D., Kim, H., 2017. LEED, Its Efficacy and Fallacy in a Regional Context—An Urban Heat Island Case in California. Sustainability 9(9), 1674.
Smid, M., Costa, A.C., 2017. Climate projections and downscaling techniques: a discussion for impact studies in urban systems. International Journal of Urban Sciences, 1-31.
Smith, C., Levermore, G., 2008. Designing urban spaces and buildings to improve sustainability and quality of life in a warmer world. Energy policy 36(12), 4558-4562.
Stewart, I.D., Oke, T.R., 2012. Local Climate Zones for Urban Temperature Studies. Bulletin of the American Meteorological Society 93(12), 1879-1900.
Street, M., Reinhart, C., Norford, L., Ochsendorf, J., 2013. Urban heat island in Boston–An evaluation of urban air-temperature models for predicting building energy use, Proceedings of BS2013: 13th Conference of International Building Performance Simulation Association. pp. 1022-1029.
Suzer, O., 2015. A comparative review of environmental concern prioritization: LEED vs other major certification systems. Journal of environmental management 154, 266-283.
Takebayashi, H., Moriyama, M., 2012. Relationships between the properties of an urban street canyon and its radiant environment: Introduction of appropriate urban heat island mitigation technologies. Solar Energy 86(9), 2255-2262.
Taleb, H., Musleh, M.A., 2015. Applying urban parametric design optimisation processes to a hot climate: Case study of the UAE. Sustainable Cities and Society 14, 236-253.
Tan, J., Zheng, Y., Tang, X., Guo, C., Li, L., Song, G., Zhen, X., Yuan, D., Kalkstein, A.J., Li, F., 2010. The urban heat island and its impact on heat waves and human health in Shanghai. International journal of biometeorology 54(1), 75-84.
Tiwari, G.N., Kumar, A., Sodha, M.S., 1982. A review—Cooling by water evaporation over roof. Energy Conversion and Management 22(2), 143-153.
Unger, J., 2004. Intra-urban relationship between surface geometry and urban heat island: review and new approach. Climate Research 27(3), 253-264.
Unger, J., 2008. Connection between urban heat island and sky view factor approximated by a software tool on a 3D urban database. International Journal of Environment and Pollution 36(1-3), 59-80.
USGBC, Reference Guide for Building Design and Construction (v4), US Green Building Council, 2014.

Wanphen, S., Nagano, K., 2009. Experimental study of the performance of porous materials to moderate the roof surface temperature by its evaporative cooling effect. Building and Environment 44(2), 338-351.
Wilcox, S., Marion, W., 2008. Users manual for TMY3 data sets. National Renewable Energy Laboratory Golden, CO.
Yang, X., Zhao, L., Bruse, M., Meng, Q., 2013. Evaluation of a microclimate model for predicting the thermal behavior of different ground surfaces. Building and Environment 60, 93-104.
Yi, Y.K., Kim, H., 2015. Agent-based geometry optimization with Genetic Algorithm (GA) for tall apartment's solar right. Solar Energy 113, 236-250.
Yi, Y.K., Kim, H., 2017. Universal Visible Sky Factor: A method for calculating the three-dimensional visible sky ratio. Building and Environment 123, 390-403.
Yi, Y.K., Malkawi, A.M., 2012. Site-specific optimal energy form generation based on hierarchical geometry relation. Automation in Construction 26, 77-91.
Yu, B., Liu, H., Wu, J., Hu, Y., Zhang, L., 2010. Automated derivation of urban building density information using airborne LiDAR data and object-based method. Landscape and Urban Planning 98(3), 210-219.
Zhao, L., Lee, X., Smith, R.B., Oleson, K., 2014. Strong contributions of local background climate to urban heat islands. Nature 511, 216.